CEAS Aeronautical Journal
https://doi.org/10.1007/s13272-025-00873-8

ORIGINAL PAPER

Integrated preliminary design of fuel cell propulsion systems for vertical take-off aircraft

Jonas Cäsar[1] · Michael Shamiyeh[2] · Daniel Weintraub[3] · Peter Jeschke[1]

Received: 30 January 2025 / Revised: 5 June 2025 / Accepted: 23 June 2025

Abstract
This paper presents a preliminary design study of a fuel cell-powered vertical take-off and landing (VTOL) aircraft. We compare the fuel cell-powered aircraft to a battery-powered aircraft and discuss the influence of key propulsion system design parameters on the aircraft mass and energy consumption. To this end, we have developed a physics-based fuel cell propulsion system design tool and coupled it with an aircraft design environment. We used the resulting integrated tool to design two four-seat VTOL aircraft with tilting propellers, one of which is powered only by batteries and the other uses PEM fuel cells supported by high-power batteries for take-off. The results show that a target aircraft mission range of 160 km is easily achievable with fuel cells, while the range with batteries alone is limited to 112 km. The fuel cell aircraft is 25 % lighter for the same payload. However, its energy consumption is 2.7 times higher, accounting for hydrogen production by electrolysis. Results of fuel cell aircraft design studies indicate that substantial oversizing of the fuel cell stack is useful to achieve low mission fuel consumption. Furthermore, the study shows that the support of the fuel cell with batteries for vertical flight phases is required to achieve a low aircraft mass and fuel consumption. In summary, we show that fuel cell propulsion systems have both advantages and disadvantages compared to battery propulsion systems for VTOL aircraft. Further, we present an integrated design method for the design of fuel cell-powered VTOL aircraft that can be used for different aircraft and mission requirements.

Keywords Preliminary design · Electric propulsion · Fuel cell · Vertical take-off aircraft

Nomenclature

C-rate	Charge rate
DC	Direct current
EASA	European Union Aviation Safety Agency
FC	Fuel cell
ISA	International standard atmosphere
MTOM	Maximum take-off mass
PEM	Polymer electrolyte membrane
PMAD	Power management and distribution
SoC	State of charge
T	Temperature
TLAR	Top-level aircraft requirements
TMS	Thermal management system
VTOL	Vertical take-off and landing

1 Introduction

In recent years, there is a growing interest in electrically powered vertical take-off and landing (VTOL) aircraft. It has been proposed that such aircraft can provide fast and sustainable transportation for people and goods in urban and suburban areas [1]. A large number of different aircraft concepts are currently being investigated and developed, often using electric propulsion systems with batteries as the sole energy source. These include the VTOL aircraft of Joby Aviation [2], Volocopter [3], and Beta Technologies [4].

There are several obstacles to the use of battery propulsion systems for VTOL aircraft. Most importantly, the energy density of batteries is low, resulting in high propulsion system masses and short aircraft ranges. The mass of electric propulsion systems can be reduced if fuel cells are used to power VTOL aircraft due to the high energy density

✉ Jonas Cäsar
caesar@ist.rwth-aachen.de

[1] Institute of Jet Propulsion and Turbomachinery, RWTH Aachen University, Templergraben 55, Aachen, Germany

[2] Bauhaus Luftfahrt e.V., Willy-Messerschmitt-Str. 1, Taufkirchen, Germany

[3] GasTurb GmbH, Melatener Straße 70, Aachen, Germany

Published online: 14 July 2025

of hydrogen. Further, hybrid propulsion systems can be used in which the fuel cell system provides the cruise power and the additional power required for take-off is supplied by a battery.

The design of electrically powered VTOL aircraft has been investigated in several studies, most of them focusing on aircraft with batteries as the sole energy source [5–8]. Design methods for tilt-wing and tilt-rotor VTOL aircraft have been presented by Palaia et al. [5] and by Jeong et al. [6], showing the potential of these aircraft configurations, but also the range limitations associated with battery propulsion systems. The potential of fuel cell propulsion systems for tilt-rotor VTOL aircraft compared to battery-powered VTOL aircraft has been investigated by Ng et al. [9] and Ahluwalia et al. [10]. Ng et al. investigated an aircraft with a take-off mass of about 3000 kg. They have shown that a battery propulsion system is advantageous in terms of propulsion system mass only for short ranges below 50 miles, while fuel cell propulsion systems are significantly lighter for longer ranges. An advantage of fuel cells over battery propulsion systems in terms of propulsion system mass was also shown by Ahluwalia et al. [10] for a four-passenger VTOL aircraft with tilt rotors and a 60-mile range. Both studies deal with hybrid propulsion systems in which the fuel cell system provides the cruise power and the additional power required for take-off is supplied by a battery. Both studies also show that the propulsion system accounts for a large share of the overall aircraft mass. Accordingly, the propulsion system design significantly influences aircraft mass and performance.

A key fuel cell propulsion system design parameter with a strong influence on system mass and efficiency is the degree of hybridization between the battery and fuel cell

$$H_P = \frac{P_{Bat}}{P_{Bat} + P_{FCS}},$$

where P_{Bat} is the installed battery power and P_{FCS} is the installed fuel cell system power. Small batteries can be used to achieve sufficient transient response times, while larger batteries can provide a significant portion of the take-off power. Park et al. [11] investigated the influence of the degree of hybridization on the propulsion system mass and performance of a two-passenger VTOL aircraft. They found that for missions with a range of 100 km, it is advantageous to supply all additional power required for take-off from a battery. For longer ranges, it is advantageous to reduce the degree of hybridization and thus the share of battery power. A lower degree of hybridization is particularly useful for tilt-rotor or lift-and-cruise aircraft, as for such configurations there is a large ratio between take-off and cruise power.

Additionally, the design current density of the fuel cell has been identified as an important design parameter affecting system mass and efficiency for conventional fuel cell-powered aircraft [12]. The current density is defined as the fuel cell current per active cell area. A high current density is required to achieve high fuel cell power. However, as the current density increases, the fuel cell voltage, and therefore the fuel cell efficiency, decreases. Due to the high efficiency at part load, the fuel cell stack is usually oversized, i.e., the design current density is set below the current density for maximum power. In addition to lower hydrogen consumption, this allows for a lighter air supply and cooling system. The optimal choice of the design current density has been investigated by Kadyk et al. [12] and Schmelcher et al. [13] for regional and short-range aircraft. To the authors' knowledge, a sensitivity study of the design current density for a VTOL aircraft application has not yet been performed in the literature.

As the aircraft design is strongly influenced by the propulsion system design, a coupled design of the propulsion system and aircraft is required for a comprehensive evaluation of fuel cell propulsion systems for VTOL aircraft. Our first goal in this paper is to evaluate fuel cell propulsion systems in comparison to battery propulsion systems with a coupled propulsion system and aircraft design approach. Our use case is a four-seat VTOL aircraft with tilt rotors as schematically shown in Fig. 1. The aircraft dimensions are derived from graphical representations of the Joby S4 aircraft [14]. Our second goal is to investigate the influence of the key fuel cell propulsion system design parameters, the degree of hybridization and the current density, on the aircraft mass and performance. For this purpose, we have developed a tool for the design and performance calculation of fuel cell propulsion systems. This tool has been integrated into the GasTurb software for aircraft propulsion system

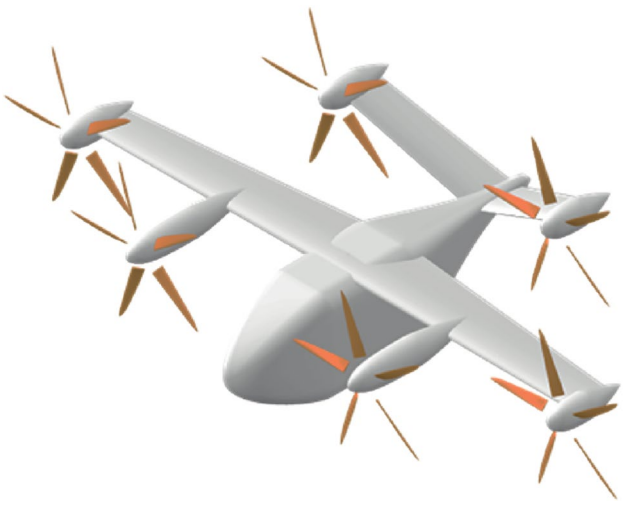

Fig. 1 Schematic of the investigated VTOL aircraft with tilt rotors in cruise configuration derived from graphical representations of the Joby S4 aircraft [14]

performance calculation [15] and coupled with a VTOL aircraft design environment. Thus, an integrated design tool for fuel cell propulsion systems for VTOL aircraft has been created.

This paper is structured as follows: First, the methodology for the integrated design of the aircraft with the individual component models is explained in detail. Next, the mission requirements and study-specific aircraft and propulsion system model parameterization are described. Finally, the results of the propulsion system and aircraft design studies are presented.

2 Methodology

This section describes the integrated preliminary design process and the modeling of the aircraft and the propulsion system with its individual components.

2.1 Integrated preliminary design process

The overall system design process, shown in Fig. 2, is divided into an aircraft design process and a propulsion system design process, each of which includes design and off-design (mission) calculations. Here, design refers to the propulsion system and aircraft sizing to meet specified mission requirements. In contrast, off-design refers to the performance calculation of the designed aircraft and propulsion system with fixed dimensions under varying operating conditions throughout the flight mission. The propulsion system design process is coupled to the aircraft design process, and both are closely connected through several interfaces.

The starting point of the overall system design is an initial design of the aircraft (fuselage, nacelles, aerodynamic surfaces) based on the prescribed top-level aircraft requirements (TLARs) with an estimate of the maximum take-off mass (MTOM). Thereby, the required design thrust of the propeller is calculated. The propeller is designed and the required shaft power and speed are calculated. In addition, initial values for the masses of the energy storage systems, the battery and hydrogen tank, are set.

The propeller shaft design power is used as basis to design the propulsion system and thereby calculate the masses and volumes of the propulsion system components. The capacities of the battery and hydrogen tank are calculated based on the previous mass estimations. The hybridization between the battery and the fuel cell and the design current density of the fuel cell are specified as design variables. These are varied in later design iterations to minimize propulsion system mass and power consumption. The resulting mass and volume of the propulsion system components are fed back into the aircraft design resulting in an MTOM that will usually not match the initial guess at first try. The design process is then repeated until the calculated aircraft mass matches the prescribed MTOM. In addition, the volumes of the propulsion system components are checked to ensure that they can be integrated into the aircraft.

Next, a mission calculation is performed to verify that the designed aircraft can achieve the specified range. The aircraft and propulsion system performance are calculated for the design mission with a time step of 10 s. At each mission point, the power requirements are transferred to the off-design calculation of the propulsion system. The hydrogen consumption and the battery discharge current are calculated for each mission point using the propulsion system off-design component models. The hydrogen mass and battery state of charge (SoC) are tracked to determine the aircraft range. If the SoC or hydrogen mass remaining in the tank at the end of the design mission are not equal to the prescribed minimum values, the battery and hydrogen tank mass are adjusted accordingly. A new aircraft and propulsion system design calculation is then performed and the mission calculation is repeated with the new design. The entire process is repeated until the specified range is achieved. Results include the mass of the aircraft and all propulsion components, the power requirements, and the energy or fuel consumption for the design mission.

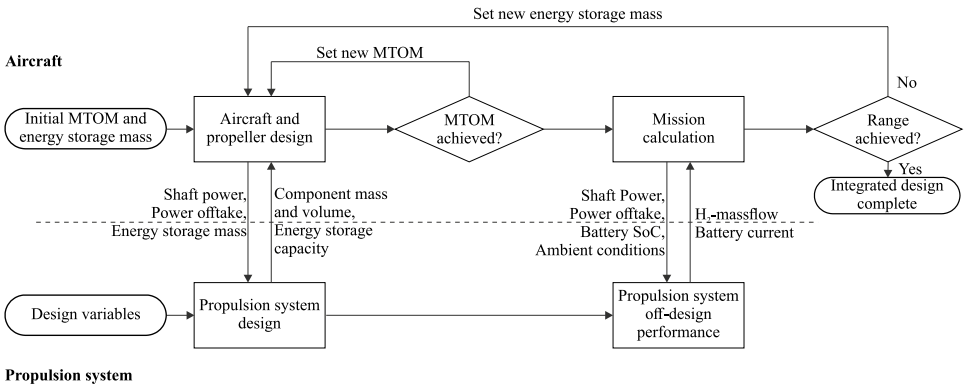

Fig. 2 Integrated preliminary design process of the aircraft and the fuel cell propulsion system

2.2 System and component modeling

This section provides an overview of the general aircraft and propulsion system models that are used to determine the performance, masses, as well as dimensions of the aircraft and propulsion system. The model input parameters for our specific VTOL application are given in section 3.2.

2.2.1 Aircraft and propeller

For aircraft design and mission analysis, a range of established conceptual design methods are used. Aerodynamics of the fixed wing and the tail plane are calculated with an adapted version of the lifting line theory [16] allowing the integration of 2D profile polars. Wing design, tail design, and propeller-rotor arrangement are based on graphical representations of the Joby S4 aircraft [14] and its geometrical dimensions are scaled to the desired aircraft size. For modeling the minimum drag coefficient CD_{min}, the component drag buildup method described by Gudmundsson [17] is used. To correctly represent the drag, the volumes of the powertrain components as well as the diameter of the electric motors are considered when designing the fuselage and nacelles. System and component masses are calculated with a combination of the statistical mass estimation methods given by Gudmundsson [17], Raymer [18] and Torenbeek [19].

The design and off-design analysis of the five-bladed variable-pitch tilt rotors is performed with XROTOR [20]. The tool calculates the axis-symmetric operating conditions of the propellers using a graded momentum formulation. The tilt rotors are modeled in hover and cruise flight only. The relatively short transition between the two flight phases is neglected for simplicity. The design of the tilt rotors follows a two-step approach. First, the propellers are designed for hover conditions with the minimum induced loss method of XROTOR. Second, the blade twist distribution is optimized to minimize energy consumption in the design mission. Propeller–wing interactions are not considered.

2.2.2 Propulsion system

Figure 3 shows schematics of the propulsion systems under investigation. The battery propulsion system consists of an electric machine, power management and distribution (PMAD) components, and a battery pack. The fuel cell propulsion system additionally features a fuel cell system that provides power during cruise flight and batteries for the support of take-off and landing flight phases. Hydrogen is supplied from a cryogenic liquid hydrogen tank. A fuel cell and battery thermal management system is included.

For the modeling of the electric machines and the PMAD components, existing methods of the GasTurb software are used, see Pohl et al. [21]. The GasTurb software has been extended with component models for the battery, fuel cell system. The hydrogen tank and thermal management systems are modeled separately and included in the propulsion system design using tabulated model result data. The component models used for the design and steady-state off-design calculations are described below.

Electric machines and power management and distribution system. Permanent magnet synchronous machines (PMSMs) are used due to their high power density and efficiency. The model allows the dimensioning and mass calculation based on machine properties such as the machine electric loading, maximum current density, maximum magnetic flux density, and mean machine density. This means that the machine power density is not constant throughout the design process, but is calculated physics-based as a function of machine speed and torque. A PMSM efficiency map is taken from [22] and used to obtain the off-design behavior of the electric machine. Thereby, differences in the machine efficiency between take-off and cruise operating points are considered in the study. The power management and distribution system (PMAD) consists of inverters, DCDC converters, power controllers, and DC cables. The inverters and DCDC converters are modeled using a simplified circuit design calculation. The efficiency of the components is calculated as a function of the semiconductor properties. The models for design and off-design calculation of the electric machines and PMAD components have been described in detail by Pohl et al. [21] and Köhler et al. [23].

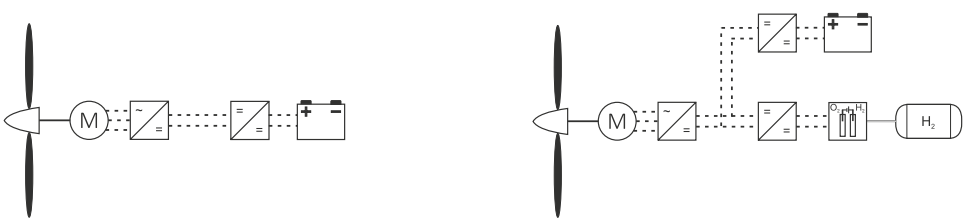

Fig. 3 Investigated propulsion systems

(a) Battery propulsion system

(b) Fuel cell propulsion system

Battery pack. The battery pack is designed as a serial and parallel combination of individual battery cells characterized by their nominal capacity, maximum discharge rate (C-rate), cell voltage, mass, and dimensions. In addition, the battery cells discharge characteristic is modeled using tabulated data of the cell voltage as a function of state of charge (SoC) and C-rate. Thereby, different battery cell designs can be accounted for. For the battery pack design, the total battery capacity, the maximum battery pack voltage, and the maximum battery pack power are given. With the nominal capacity and maximum C-rate of each cell, the number of battery cells in series and parallel and thereby the mass and volume are calculated. During the off-design calculation, the respective SoC and the power demand are inputs to the cell model. The output is the battery pack current, which is then used to calculate a new SoC. A detailed description of the battery model is given by Köhler et al. [23].

Fuel cell system. A low-temperature polymer electrolyte membrane fuel cell (PEMFC) is considered in this study. The fuel cell system consists of the fuel cell stack and an air supply system as shown schematically in Fig. 4.

The fuel cell model is based on the established electrochemical equations to determine the performance of a single cell [24]. The model takes into account the characteristic loss mechanisms in proton exchange membrane fuel cells as a function of current density and operating pressure. The other operating parameters, temperature, humidity, and stoichiometry, are set constant. The fuel cell model is calibrated using cell data from O'Hayre et al. [24] as well as publicly available data on the Toyota Mirai fuel cell stack [25]. An operating temperature of 80 °C, a cathode inlet relative humidity of 80 % and an air stoichiometry of 2 are set. The resulting polarization curves are shown in Fig. 5. To design the fuel cell stack, first the current density and operating pressure of the fuel cell at the design point are specified and the cell voltage is calculated. On this basis, the number of cells in the stack to provide the demanded power and thereby the mass and volume of the stack are determined.

The air supply system conditions ambient air to meet the requirements at the fuel cell cathode inlet. To achieve this, the ambient air is first compressed in an electrically assisted turbocharger, then cooled in an aftercooler, and finally humidified in a membrane humidifier. A turbine downstream

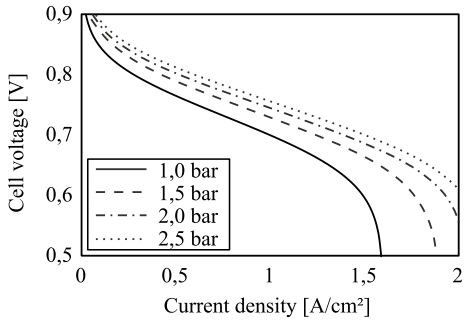

Fig. 5 Fuel cell polarization curves for four different operating pressures

of the fuel cell cathode recovers some of the compression power. The required air mass flow is calculated using Faraday's law. Compressor and turbine power, aftercooler heat flux and humidifier membrane water mass flow are calculated using basic thermodynamic equations. The masses of the air supply system components are determined using flow specific factors. The aftercooler mass is calculated as part of the thermal management system. Scaled component maps are used for the off-design calculation of the turbocharger [26].

Hydrogen tank. The hydrogen tank is designed as a cryogenic liquid tank with foam insulation using the model of Lin et al. [27]. The mass of hydrogen to be stored in the tank is an input parameter to the model. In addition, a maximum pressure in the tank and a maximum time until this pressure is reached and hydrogen must be released are set as inputs. As a result, the mass of the tank, the external volume of the tank and the storage density are determined. The material parameters for the foam insulation are taken from Brewer [28]. The required aluminum wall thickness of the pressure vessel is determined based on calculation guidelines from [29]. The required insulation thickness is calculated using 1D heat transfer equations.

Thermal management system. Thermal management systems (TMS) are considered for the battery and for the fuel cell system. The TMS is sized for hot day take-off conditions ($\Delta T_{ISA} = +25$ K). Due to the low operating temperature of batteries, thermoelectric modules capable of cooling below ambient temperature in combination with a

Fig. 4 Fuel cell system

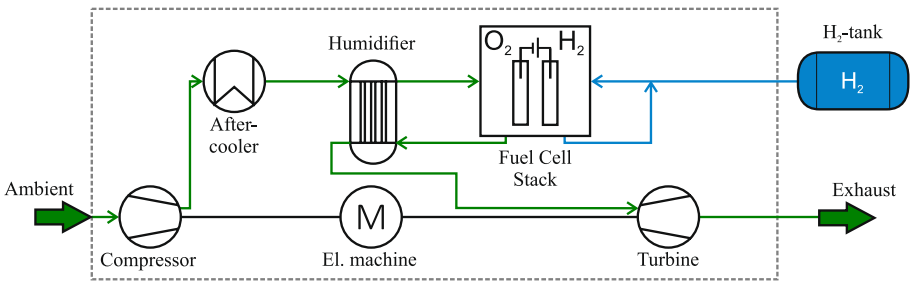

ram air heat exchanger are used for battery cooling. The modeling of the TMS architecture has been presented by Kellermann et al. in a previous publication [30]. For the fuel cell a liquid cooling system is used. The cooling fluid collects heat from the two main heat sources, the fuel cell stack and the compressor aftercooler. The heat is then dissipated in a ram air heat exchanger. Details on the modeling of the heat exchangers can be found in [31]. A cooling fan is used to provide sufficient cooling air flow during vertical and cruise flight. Additional drag due to the cooling system is not considered in the studies. Both the battery and fuel cell TMS models show a linear relationship between waste heat and TMS mass and power requirements. Therefore, heat specific factors can be generated from the models and used for the overall design process.

3 Aircraft design study

In this section, we present the preliminary design of the VTOL aircraft with battery and fuel cell propulsion system. We then compare the fuel cell-powered aircraft to the battery-powered aircraft with regard to their range, mass, and energy consumption.

3.1 Requirements

The TLARs used for this study are listed in Table 1. They apply to a four-seat aircraft and are based on current VTOL aircraft concepts and a market study by Uber Elevate [1]. A four-seat aircraft with a payload of 440 kg, a design range of of 160 km, and cruise speed of 240 km/h is studied here. A stopover within the design range without battery recharge or hydrogen refueling is assumed. This stopover provides a high degree of operational flexibility and allows transportation from the city to outlying areas where the necessary infrastructure for recharging or refueling may not be available. For each take-off or landing, a 30 s hover phase is accounted. Due to the limited space at landing sites in urban areas, a maximum wingspan of 15.25 m is specified for the aircraft. An MTOM of 3175 kg is set as an upper limit for the aircraft design based on the EASA Special Condition VTOL 01 [32]. The same TLARs are used for both the battery and the fuel cell-powered aircraft. The fuel cell-powered aircraft is initially designed so that the fuel cell system provides the cruise power and the battery provides all the additional power, required for take-off. For the studies in this paper, technology assumptions are made for a year of entry into service in 2035.

Table 1 Top-level aircraft requirements

Payload	440	kg
Cruise speed	240	km/h
Range	160	km
Diversion	10	km
Cruise altitude	500	m
Service ceiling	3000	m
Hover duration	30	s
Span	≤15.25	m
MTOM	≤ 3175	kg
Year of entry into service	2035	

Failure safety is considered throughout the aircraft and propulsion system design process. It is required that the failure of one propeller is tolerated at any point of the flight mission. The loss of a single propeller, for example due to bird strike, material fatigue, or an electric machine failure, can never be ruled out. To prevent a roll moment resulting from the failure, the other propellers on the same side of the aircraft must be able to provide more power accordingly. The total number of propellers on the aircraft is set at six for the overall system studies. This number allows for a small oversizing of the propellers and its motors, while still allowing for large propellers to maintain high propeller efficiency.

Power supply redundancies have been introduced as well. The aircraft are equipped with three independent DC buses that supply power to opposite propellers on the aircraft. Each propeller can be powered by two different DC buses, so that one bus can safely fail. In both the battery and fuel cell-powered aircraft, each DC bus is powered by one battery pack. In the fuel cell aircraft, an additional fuel cell system supplies power to all DC buses. The system is designed to compensate for a failure of a battery pack or the fuel cell system during vertical flight. In combination with an aborted landing, it is stipulated that the aircraft must still be able to fly a diversion of 10 km after any component failure. We consider these requirements necessary to achieve safe operation of VTOL aircraft in urban environments. This also means that the batteries of the fuel cell-powered aircraft must be large enough to provide the energy and power for the 10 km diversion in case of a fuel cell failure. This scenario thus also serves as the design point for the batteries and the fuel cell system in the design process. The resulting propulsion system architecture is shown schematically in Fig. 6.

3.2 Aircraft, system, and component design

In this section, we present the aircraft, system and component design parameters and accompanying assumptions. The modeling methods are parameterized and calibrated for the specific VTOL aircraft use case investigated in this paper.

For the aircraft design, the dimensions of the aircraft are derived from graphical representations of the Joby S4 aircraft [14] and scaled to match the maximum allowed span listed in Table 1. The diameter of all tilt rotors is

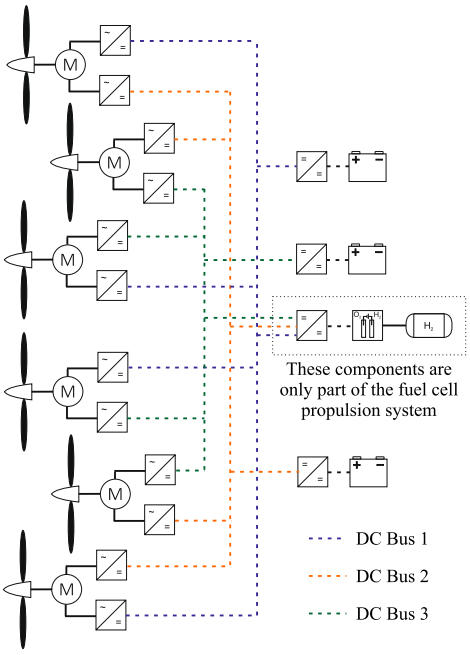

Fig. 6 Fail-safe propulsion system architecture

evenly increased, while the rotor arrangement on the aircraft is preserved. The length of the wing root chord as well as the taper ratio is kept constant. This increases the aspect ratio of the wing and improves cruise efficiency. The fuselage length is adjusted to accommodate the four passenger seats and, depending on the configuration, either the battery packs or the fuel cell system with the liquid hydrogen tank and the respective power management and distribution components (see Fig. 10). This allows for short hydrogen lines and a compact electric system design. The propeller nacelles are designed to accommodate the electric machines with the appropriate diameter and installation space. Table 4 in the Appendix lists the aircraft dimensions used for the aircraft design in this study.

The propeller rotor tip speed is limited to a Mach number of 0.5 for regular operation to ensure reduced noise emissions. A maneuvering thrust reserve of 15 % is added to the design thrust. Due to the low propeller speed and the lack of a gearbox, the electric machines are designed for low speed and high torque. The parametrization of the electric machine model is based on high torque machines from MAGicALL (MAGiDRIVE product line) [33] and typical electric machine design parameters from Binder et al. [34]. The mean machine density is first calibrated to match the masses of the MAGicALL machines, and then a 10 % density reduction is assumed for the year of entry into service 2035. The design parameters are listed in Table 5 in the Appendix. The component model

Table 2 Key technology assumptions for the battery-powered and the fuel cell-powered aircraft

	Battery-powered aircraft	Fuel cell-powered aircraft
Max. battery pack power density	1.28 kW/kg	2.7 kW/kg
Battery pack energy density	320 Wh/kg	180 Wh/kg
Max. fuel cell stack power density	-	3.0 kW/kg

parametrization for the inverters, DCDC converters, and DC cables within this study is taken from Pohl et al. [21]. The DC voltage is fixed at 800 V.

The two propulsion systems use different types of battery cells. For the battery propulsion system, the capacity requirement determines the size of the battery, as it must provide the full mission energy. In this case, a cell optimized for high energy density and a low maximum C-rate of 4 was selected [35]. The fuel cell aircraft, on the other hand, uses a battery optimized for a high power density because it needs to support the short power peaks during take-off and landing. Accordingly, the cell data was taken from a battery cell with a high maximum C-rate of 15 [36]. An end-of-life capacity of 90 % of the initial capacity is considered for both battery types. The minimum SoC at the end of the design mission is set to 15 %. The mass of the battery cells is calibrated using a factor on the cell mass to meet the assumed energy and power densities for the year 2035, as listed in Table 2. The design inputs and heat specific factors for the battery TMS design are listed in Table 6.

The mass of the fuel cell stack is calibrated by applying a factor to the cell mass to achieve the assumed stack level power density listed in Table 2 at a current density of 2.0 A/cm^2 and an operating pressure of 2.5 bar. Taking into account the air supply system and the thermal management system mass, the current density for a minimum fuel cell system mass is 1.4 A/cm^2, which is about 80 % of the maximum stack power. The air supply compressor design pressure ratio is set to 2.6 for overall high system efficiency. The design and operation of the air supply system will be addressed in future publications. Additional design data for the air supply system as well as the heat specific factors for the fuel cell TMS design can be found in Table 7 in the Appendix.

The liquid hydrogen tank is designed for a 2-h period before hydrogen must be vented due to rising pressure inside the tank. Additional heat flux into the tank and mass from tank instrumentation and valves are taken from Ladous et al. [37]. A 10 % hydrogen reserve is assumed for the tank design. Hydrogen tank design results are given in Fig. 11.

3.3 Design results

The design results for both aircraft are presented in Table 3. The target range of 160 km is easily realized with the fuel cell-powered aircraft and at an MTOM of only 2409 kg. The battery-powered aircraft, by contrast, reaches the upper limit for the MTOM of 3175 kg at a design range of 112 km. It is hence unable to fulfill the 160 km range requirement with the given design assumptions for a 2035 entry into service.

The aircraft design is strongly influenced by the cascading effects of the propulsion system mass. Lower propulsion system and energy carrier masses reduce the aircraft mass, which results in a lower design power for the propulsion system and in turn reduces the propulsion system and energy carrier mass. This effect is amplified by the lower disk loading of a lighter aircraft. Therefore, the mass of the electric machines and PMAD in the fuel cell-powered aircraft is 32 % lower than in the battery-powered aircraft. Overall, these effects result in a propulsion system mass that is about 38 % lighter when using fuel cells even though the battery-powered aircraft fails to meet the range requirement. In addition, it should be noted that the hydrogen tank weighs only about 4 % of the fuel cell aircraft MTOM (including hydrogen). Increasing the size of the hydrogen tank has little effect on the overall aircraft mass, hence a significantly greater range is easily achieved. The fuel cell system is designed to provide the propeller cruise power of 206 kW. The degree of hybridization between the installed battery and the fuel cell system power is 0.69. Including the thermal management system, the battery achieves a higher power density than the fuel cell system. Therefore, reducing the battery power and increasing the fuel cell system power would result in an increase in propulsion system and aircraft mass. The presented fuel cell aircraft design is therefore also the design for minimum system mass.

Since the two aircraft use different energy carriers, the energy consumption cannot be directly compared. If the hydrogen is produced by electrolysis, the results can be evaluated in terms of electrical energy consumption. For electrolysis, an efficiency of about 70 % and for liquefaction and transport of hydrogen, an efficiency of 83 % can be assumed based on the lower heating value of hydrogen [38]. This gives an energy consumption of 395 kWh/100 km for the fuel cell-powered aircraft. This is 2.7 times higher compared to 145 kWh/100 km for the battery-powered aircraft. The reduction in propulsion system and aircraft mass compared to a battery-powered aircraft can therefore not overcompensate for the high energy losses in hydrogen generation, liquefaction and conversion in fuel cells when looking at overall energy consumption.

Further, failure scenarios significantly affect the results. As described in Section 3.1, the propulsion system must be able to provide sufficient thrust in the event of propeller, battery or fuel cell failure during a vertical flight phase. Additionally, it needs to provide enough energy for a 10 km diversion after the failure. As a result, the electric machines installed power listed in Table 3 is significantly higher than

Table 3 Results of the overall aircraft design

	Battery-powered aircraft	Fuel cell-powered aircraft
Range (without 10 km diversion)	112 km	160 km
MTOM	3175 kg	2409 kg
Payload	440 kg	440 kg
Structure and landing gear mass	705 kg	589 kg
Aircraft systems mass	188 kg	167 kg
Seats and furnishing mass	58 kg	58 kg
Propulsion system mass	1657 kg	1027 kg
Electric machines	187 kg	137 kg
Power management and distribution	301 kg	195 kg
Battery mass	979 kg	219 kg
Fuel cell stack and air supply system	-	179 kg
Thermal management system	190 kg	206 kg
Hydrogen tank mass (filled)	-	98 kg
Variable pitch propellers mass	128 kg	128 kg
Energy/fuel consumption	145 kWh/100 km	6.8 kg_{H_2}/100 km
Installed power	1278 kW	858 kW
Hovering power	574 kW	403 kW
Cruise power	250 kW	206 kW
Propeller diameter	3.4 m	3.4 m
Disk loading	58 kg/m^2	44 kg/m^2

the required hover power if no failure occurs. The masses of the electric machines and the PMAD increase accordingly. High battery power and capacity reserves are required for fuel cell system or battery pack failure as well as for the diversion. At the end of the design mission, the battery SoC of the fuel cell aircraft is 67 % and of the battery-powered aircraft is 28 %. The large reserves of electric machine power and battery energy indicate that failure scenarios have significantly influenced the aircraft design process and should be considered for a meaningful evaluation of VTOL aircraft.

3.4 Design sensitivities

The system design in the previous section aimed for a minimum overall mass of both battery and fuel cell-powered aircraft. For the battery-powered aircraft, lowest mass entails minimum energy consumption. For the fuel cell-powered aircraft this is not necessarily the case. There are two key fuel cell system design parameters so far set constant, that greatly affect system mass and energy consumption, these being the design current density of the fuel cell stack and the hybridization between fuel cell and battery power. These are investigated here based on the previously described design of the fuel cell-powered aircraft from Table 3 as the reference design. Several new aircraft designs are conceived by varying the design point current density and degree of hybridization and then repeating the overall system design process described in Section 2.1. All TLARs listed in Table 1 still apply to the adapted aircraft designs.

3.4.1 Fuel cell design current density

As described in the introduction, the design current density determines the size of the fuel cell stack. As the fuel cell design current density is reduced, a greater number of fuel cells are required to achieve the same design power, increasing the mass of the fuel cell stack. The advantage of a low design current density is a high fuel cell efficiency.

Figure 7a shows the change of propulsion system mass, fuel cell system mass and cruise fuel consumption relative to the reference design as a function of the fuel cell design current density. The propulsion system mass includes the mass of the electric machines, PMAD, fuel cell system, and batteries including cooling systems. The fuel flow is calculated at off-design cruise conditions. The installed propulsion system power and cruise power requirements are held constant. Reducing the design current density from the reference 1.4 A/cm^2 to 0.6 A/cm^2 results in a significant cruise fuel flow reduction of 16 %. However, this also leads to a 35 % increase in fuel cell system mass and 11 % increase in propulsion system mass. The reason for the increasing mass is the oversizing of the fuel cell stack with an increasing number of cells for the same power at a lower current density. This effect dominates the mass reduction of both the air supply system and the cooling system, due to the rising fuel cell efficiency for lower than 1.4 A/cm^2 current density. As a result of the opposing trends for mass and energy consumption, no choice of the current density for minimum mission energy consumption can be made when looking at the propulsion system. The influence of the propulsion system mass on the aircraft power demand must be taken into account, e.g., like we do with the integrated design process of this paper.

The influence of the design current density on aircraft mass and mission fuel consumption is shown in Fig. 7b. A reduction of the design current density from the reference design at 1.4 A/cm^2 results in a growing aircraft mass due to the rising propulsion system mass and, accordingly, a

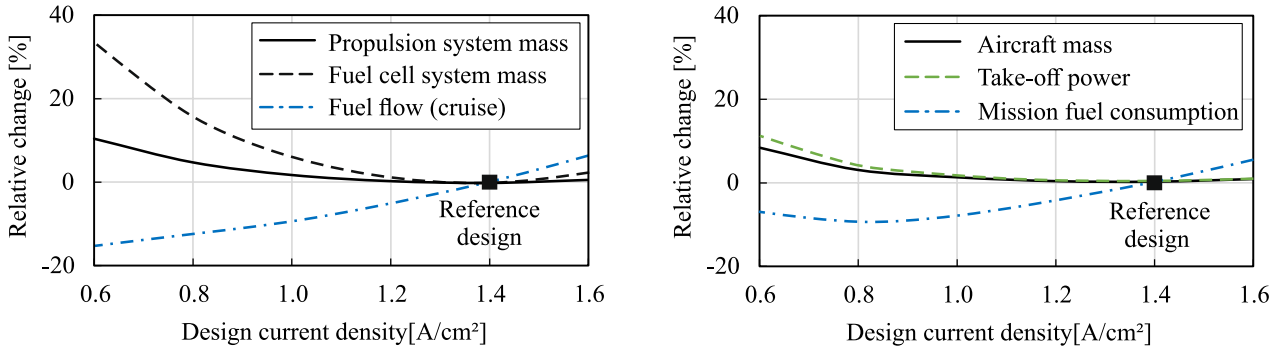

(a) Propulsion system mass, fuel cell system mass (without hydrogen tank) and cruise fuel flow at constant propulsion system power

(b) Aircraft mass, take-off power and mission fuel consumption

Fig. 7 Influence of the design current density on the propulsion system mass and performance and on the aircraft mass and performance relative to the reference design

growing take-off power. Interestingly however, the aircraft mass shows little sensitivity with regard to the design current density with only about 3 % higher aircraft mass at a design current density of 0.8 A/cm^2, which corresponds to a signifiant fuel cell stack oversizing. At this point, a 9 % reduction of the mission fuel consumption is achieved compared to the reference design. Below 0.8 A/cm^2, the rising energy requirements due to higher aircraft mass dominate the efficiency gains. Sensible values for the design current density can therefore be selected in a relatively wide range between a current density of 0.8 A/cm^2 and 1.4 A/cm^2 with an optimum in terms of mission fuel consumption at 0.8 A/cm^2. The conclusion is that even for highly mass-sensitive flight applications, a low design current density and thereby significantly oversized fuel cell stack is advantageous due to the efficiency gains.

3.4.2 Degree of hybridization

The fuel cell system of the reference aircraft is sized for cruise power and the battery is sized to provide any additional power needed for vertical flight and in the event of fuel cell system failure. A study is now being conducted to determine how changing the described hybridization between fuel cell and battery power affects the system mass and fuel consumption. The degree of hybridization for the reference design is 69 %. When changing the degree of hybridization, it is important that sufficient power redundancies are maintained. Increasing the power of the fuel cell system and reducing the power of the three batteries of the reference design changes the ratio of power lost if one of the component fails. To obtain the same power redundancy constraints as the reference design, and to avoid confounding the results with the influence of the failure scenarios,

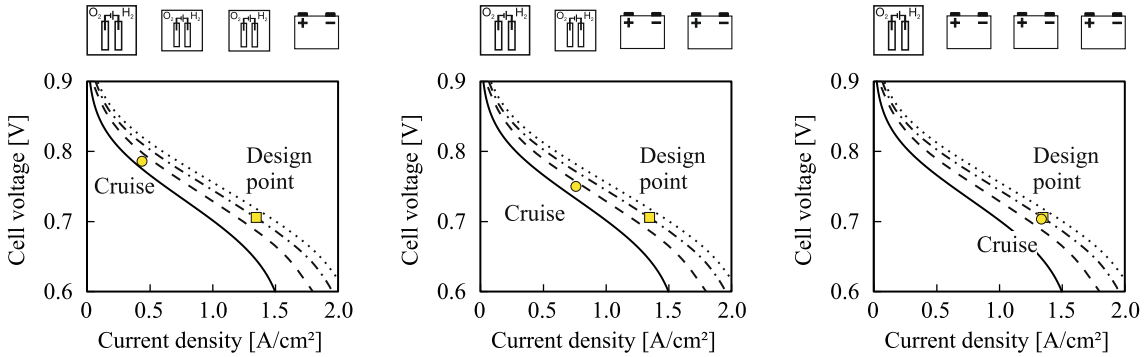

(a) $H_P = 23\,\%$ (b) $H_P = 46\,\%$ (c) $H_P = 69\,\%$ (Reference)

Fig. 8 Influence of the design degree of hybridization H_P on the fuel cell cruise operating point

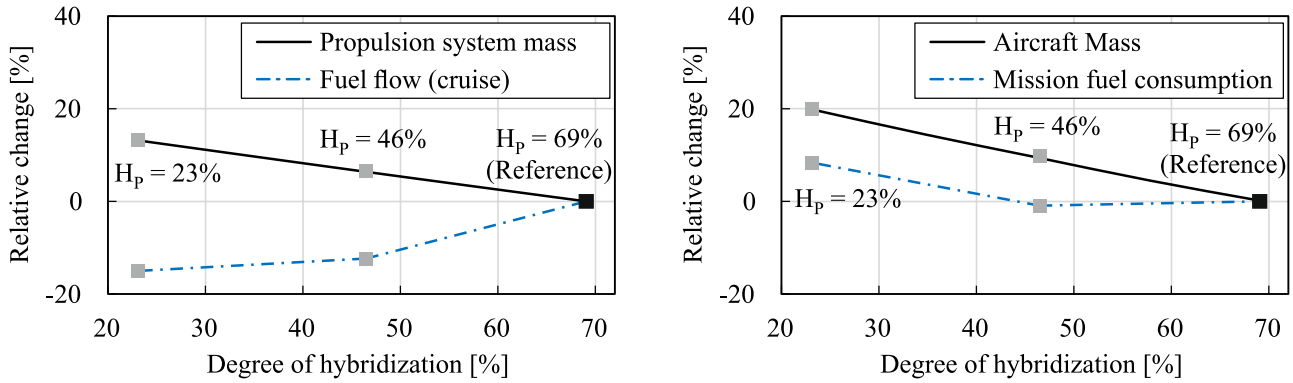

(a) Propulsion system mass, fuel cell system mass (without hydrogen tank) and cruise fuel flow at constant propulsion system power

(b) Aircraft mass and mission fuel consumption

Fig. 9 Influence of the degree of hybridization on the propulsion system mass and performance and on the aircraft mass and performance relative to the reference design

the analysis is performed for discrete degrees of hybridization, where each battery is replaced by a fuel cell system ($H_P = 46\,\%$ and $H_P = 23\,\%$). Fig. 8 shows the influence of the degree of hybridization on the current density of the fuel cell. A lower degree of hybridization ($H_P = 46\,\%$ and $H_P = 23\,\%$) results in a lower cruise current density and a higher cell voltage when the design current density is kept constant. Therefore, sizing the fuel cell for vertical flight and operating the fuel cell at part load during cruise can be advantageous in terms of mission fuel consumption while at the same time reducing battery mass.

The influence of the of hybridization on the propulsion system mass and cruise fuel flow is shown in Fig. 9a. The propulsion system power and cruise power requirements are held constant here. As the degree of hybridization decreases, the cruise fuel flow decreases due to the higher cell voltage at part load. At a degree of hybridization of 23 %, the cruise fuel flow is reduced by 15 % compared to the reference design. However, the propulsion system is 13 % heavier than the reference design. This is due to an increase in fuel cell system mass, which overcompensates for the reduction in battery mass as the battery achieves a higher power density than the fuel cell system, once the additional mass of the air supply and thermal management system is taken into account.

The influence of a decreasing degree of hybridization on the aircraft level is shown in Fig. 9b. The changing propulsion system and aircraft mass are now considered in the power requirements. To calculate the results shown, interpolations of the structural mass fraction and the lift-to-drag ratio between VTOL designs with different MTOM have been performed. Reliable results can be obtained with this method due to the generally linear relationship between the MTOM and the structural mass fraction of the aircraft and the lift-to-drag ratio. Reducing the degree of hybridization to 46 % results in lower mission fuel consumption due to the higher fuel cell efficiency at cruise power requirements. However, the reduction in fuel consumption is only 1 % and the aircraft becomes 9 % heavier. Despite the higher efficiency of the fuel cell, further reducing the degree of hybridization to 23 % does not result in a continued reduction in mission fuel consumption. The mission fuel consumption increases by 7 % compared to the reference design due to the high mass and power requirements of the aircraft.

For the given application, we conclude that it is not only advantageous but also necessary to support the vertical flight with high power density batteries. Due to the high aircraft design sensitivity to the propulsion system mass, it is sensible to use a battery for the entire additional vertical flight power ($H_P = 69\,\%$). The result highly depends on the power densities of the battery and fuel cell stack. A smaller difference between the power densities would lead to a smaller increase in the mass of the propulsion system when changing the degree of hybridization. This could change the outcome of this study. Additionally, in a VTOL application the ratio between take-off and cruise power is naturally high and the range of the design mission is low. For aircraft applications with a lower take-off to cruise power ratio or higher ranges, we expect that the optimum design will shift to lower degrees of hybridization or no hybridization at all.

4 Summary

The results presented above highlight the advantages and drawbacks of using fuel cells for VTOL aircraft propulsion. For the given VTOL application, the battery-powered aircraft can achieve a maximum range of 112 km. In contrast, the fuel cell aircraft achieves the target range of 160 km and is also 25 % lighter than the battery powered aircraft for the same payload. However, the energy consumption of the fuel cell-powered aircraft is 2.7 times higher when using hydrogen from electrolysis. This is due to the high losses in the production of hydrogen and its conversion in the fuel cell. It can therefore be concluded that fuel cells are required for high VTOL aircraft ranges, but for low ranges, sole battery propulsion is preferable due to its by far lower energy consumption and thus lower operating costs. The results additionally show the importance of including failure scenarios for a sensible evaluation. For the given application, the propeller design power is 80 % higher when considering sufficient failure safety.

The studies also highlight the importance of a coupled propulsion system and aircraft design process. This is mainly due to the high proportion of propulsion mass in the overall aircraft mass. For the fuel cell-powered aircraft it is shown that a significant oversizing of the fuel cell stack, i.e., a low design current density, is useful to achieve low mission fuel consumption. For the given application a 9 % reduction in mission fuel consumption can be achieved compared to a design for minimum aircraft system mass. Furthermore, the study shows that it is sensible to provide the additional power required for vertical flight from batteries to achieve a low aircraft mass and fuel consumption. This is because batteries can achieve higher power densities than fuel cell systems.

In conclusion, the optimal propulsion system design can only be found using a coupled aircraft and propulsion system design methodology. The integrated design method presented in this paper allows the evaluation of fuel cell propulsion systems and also provides a basis for investigating other aircraft applications and mission requirements.

Appendix A Aircraft, system, and component parametrization

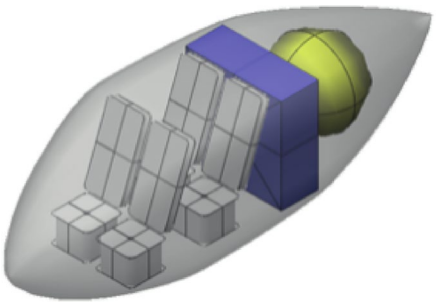

Fig. 10 Fuselage geometry and internal layout of the fuel cell aircraft configuration featuring four passenger seats, a placeholder for the fuel cell system and power management and distribution (blue) and the liquid hydrogen tank (yellow)

Table 4 Aircraft geometry data

Parameter	Unit	Extracted data from [14]	Scaled aircraft
Wing			
Span (without propeller)	m	10.7	11.84
Root chord length	m	1.63	1.63
Tip chord length	m	0.75	0.75
Taper ratio	-	0.46	0.46
Aspect ratio	-	8.24	9.4
Tilt-rotor diameter	m	3.12	3.4
Rotor area (total)	m^2	45.94	54.5
Fuselage			
Max. width	m	1.65	1.6
Height	m		1.8

Table 5 Electric machine design data

Parameter	Value	Unit
Electric loading	112	kA/m
Max. current density	9	A/mm^2
Air gap peak flux density	0.89	T
Mean machine density	1123	kg/m^3
Copper fill factor	0.75	
Winding factor	0.945	
Power factor	0.82	
Design efficiency	96.5	%
Number of pole pairs	5	
Active length to air gap diameter ratio	0.78	

Table 6 Battery and battery TMS design data

Parameter	Value	Unit
Minimum SoC	0.15	
Maximum SoC	0.9	
Max. C-rate high power density cell	15.0	
Max. C-rate high energy density cell	4.0	
Battery TMS heat specific mass	3.6	kg/kW_Q
Battery TMS heat specific power	0.84	kW/kW_Q

Table 7 Fuel cell air supply system and fuel cell TMS design data

Parameter	Value	Unit
Air intake pressure ratio	0.98	
Compressor pressure ratio	2.6	
Aftercooler pressure ratio	0.95	
Humidifier dry side pressure ratio	0.95	
Humidifier wet side pressure ratio	0.95	
Fuel cell cathode pressure ratio	0.9	
Compressor efficiency	0.8	
Turbine efficiency	0.85	
Humidifier flow specific mass	75	kg/(kg/s)
Compressor flow specific mass	10	kg/(kg/s)
Turbine flow specific mass	10	kg/(kg/s)
Fuel cell TMS heat specific mass	0.42	kg/kW_Q
Fuel cell TMS heat specific power	0.19	kW/kW_Q

Table 8 Cryogenic liquid hydrogen tank design data

Parameter	Value	Unit
Length to diameter ratio	1.0	
Time until hydrogen boil-off ventilation	2.0	h
Hydrogen filling pressure	1.2	bar
Max. pressure	8.0	bar
Auxiliary component heat flux	5.8	W
Auxiliary component mass	58	kg

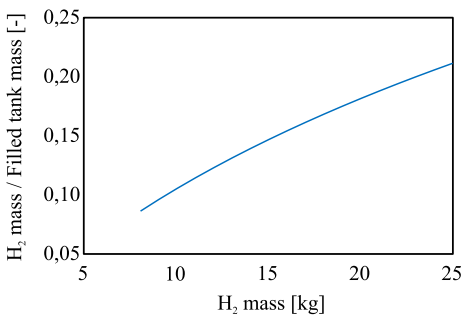

Fig. 11 Cryogenic liquid hydrogen tank gravimetric efficiency (H_2-mass/filled tank mass) as a function of the H_2-mass calculated with the design parameters in Table 8

Acknowledgements We would like to thank Hagen Kellermann, Jo Köhler and Markus Pohl for their dedication to the success of the IVekLu project and their support for this publication.

Funding Open Access funding enabled and organized by Projekt DEAL. This research received funding as part of the IVekLu project, a research project supported by the Federal Ministry for Economics and Climate Action in the German Aviation Research Program. Open Access funding enabled and organized by Projekt DEAL. Open Access funding enabled and organized by Projekt DEAL.

Declarations

Competing interest The authors have no competing interests to declare that are relevant to the content of this article.

Data availability Data sets generated during the current study are available from the corresponding author on reasonable request.

References

1. Uber Elevate: Fast-Forwarding to a Future of On-Demand Urban Air Transportation, (2016)
2. Joby Aviation: Joby Aviation - Our Story. [Accessed 15 February 2024]. https://www.jobyaviation.com/about/
3. Volocopter GmbH: Volocopter Completes Production Setup for Electric Air Taxis. [Accessed 05 April 2024]. https://www.volocopter.com/newsroom/volocopter-completes-production-setup/
4. Beta Technologies: The ALIA Platform. [Accessed 17 January 2024]. https://www.beta.team/aircraft/
5. Palaia, G., Abu Salem, K., Cipolla, V., Binante, V., Zanetti, D.: A conceptual design methodology for e-vtol aircraft for urban air mobility. Appl. Sci. **11**(22), 10815 (2021). https://doi.org/10.3390/app112210815
6. Jeong, T., Radotich, M., Johnson, W., Silva, C.: Design of a six-tiltrotor concept vehicle for urban air mobility (2024). https://doi.org/10.2514/6.2024-4427
7. Xiao, J., Salk, N., Haran, K.: Conceptual design of an evtol air shuttle for rapid intercity transport, 1–8 (2020) https://doi.org/10.1109/PECI48348.2020.9064631
8. Cole, J.A., Rajauski, L., Loughran, A., Karpowicz, A., Salinger, S.: Configuration study of electric helicopters for urban air mobility. Aerospace **8**(2), 54 (2021). https://doi.org/10.3390/aerospace8020054
9. Ng, W., Datta, A.: Hydrogen fuel cells and batteries for electric-vertical takeoff and landing aircraft. J. Aircraft **56**(5), 1765–1782 (2019). https://doi.org/10.2514/1.C035218
10. Ahluwalia, R.K., Peng, J.-K., Wang, X., Papadias, D., Kopasz, J.: Performance and cost of fuel cells for urban air mobility. Int. J. Hydrogen Energy **46**(74), 36917–36929 (2021). https://doi.org/10.1016/j.ijhydene.2021.08.211
11. Park, J., Lee, D., Lim, D., Yee, K.: A refined sizing method of fuel cell-battery hybrid system for evtol aircraft. Appl. Energy **328**, 120160 (2022). https://doi.org/10.1016/j.apenergy.2022.120160
12. Kadyk, T., Winnefeld, C., Hanke-Rauschenbach, R., Krewer, U.: Analysis and design of fuel cell systems for aviation. Energies **11**(2), 375 (2018). https://doi.org/10.3390/en11020375
13. Schmelcher, M., Häßy, J.: Hydrogen fuel cells for aviation? a potential analysis comparing different thrust categories. ISABE (2022)
14. The Vertical Flight Society: Electric VTOL News - Joby S4. [Accessed 08 February 2024]. https://evtol.news/joby-s4
15. GasTurb GmbH: GasTurb 14 Manual, (2022)
16. Phillips, W.F., Snyder, D.O.: Modern adaptation of prandtl's classic lifting-line theory. J. Aircraft **37**(4), 662–670 (2000). https://doi.org/10.2514/2.2649
17. Gudmundsson, S.: General Aviation Aircraft Design: Applied Methods and Procedures, Second edition edn. Butterworth-Heinemann an imprint of Elsevier, Oxford and Cambridge (2022). https://doi.org/10.1016/C2018-0-03861-X
18. Raymer, D.P.: Aircraft Design: A Conceptual Approach. AIAA education series. American Institute of Aeronautics and Astronautics, Washington, DC (1996)
19. Torenbeek, E.: Synthesis of Subsonic Airplane Design. Springer, Netherlands, Dordrecht (1986)
20. Drela, Mark: XROTOR (2011). https://web.mit.edu/drela/Public/web/xrotor/
21. Pohl, M., Köhler, J., Kellermann, H., Lüdemann, M., Weintraub, D., Jeschke, P., Hornung, M.: Preliminary design of integrated partial turboelectric aircraft propulsion systems. J. Global Power Propulsion Soc. **6**, 1–23 (2022). https://doi.org/10.33737/jgpps/145907
22. Pellegrino, G., Vagati, A., Boazzo, B., Guglielmi, P.: Comparison of induction and pm synchronous motor drives for ev application including design examples. IEEE Trans. Indus. Appl. **48**(6), 2322–2332 (2012). https://doi.org/10.1109/TIA.2012.2227092
23. Köhler, J., Jeschke, P.: Conceptual design and comparison of hybrid electric propulsion systems for small aircraft. CEAS Aeron. J. **12**(4), 907–922 (2021). https://doi.org/10.1007/s13272-021-00536-4
24. O'Hayre, R.P., Prinz, F.B., Cha, S.-W., Colella, W.G.: Fuel Cell Fundamentals. Wiley, Hoboken (2016)
25. Lohse-Busch, H., Stutenberg, K., Duoba, M., Iliev, S.: Technology Assessment Of A Fuel Cell Vehicle: 2017 Toyota Mirai (2018). https://doi.org/10.2172/1463251
26. Kurzke, Joachim: Compressor and Turbine Maps for Gas Turbine Performance Computer Programs, Garrett T-Series T61 Turbocharger, Issue 3 edn. GasTurb GmbH
27. Lin, C.S., van Dresar, N.T., Hasan, M.M.: Pressure control analysis of cryogenic storage systems. J. Propulsion Power **20**(3), 480–485 (2004). https://doi.org/10.2514/1.10387
28. Brewer, G.D.: Hydrogen Aircraft Technology. CRC Press, Boca Raton (1991)
29. Dampfkesselausschuss, Deutscher: Technische Regeln für Dampfkessel. Verband der TÜV e.V, Berlin (2010)
30. Kellermann, H., Fuhrmann, S., Shamiyeh, M., Hornung, M.: Design of a battery cooling system for hybrid electric aircraft. J. Propulsion Power **38**(5), 736–751 (2022). https://doi.org/10.2514/1.B38695
31. Kellermann, H., Lüdemann, M., Pohl, M., Hornung, M.: Design and optimization of ram air-based thermal management systems for hybrid-electric aircraft. Aerospace **8**(1), 3 (2021). https://doi.org/10.3390/aerospace8010003

32. European Union Aviation Safety Agency: Special Condition Vertical Take-Off and Landing (VTOL) Aircaft. https://www.easa.europa.eu/sites/default/files/dfu/SC-VTOL-01.pdf
33. MAGicALL: Integrated Motor | Controller: MAGiDRIVE™. [Accessed 19 December 2023]. https://www.magicall.biz/products/integrated-motor-controller-magidrive/
34. Binder, A.: Elektrische Maschinen und Antriebe. Springer, Berlin Heidelberg, Berlin, Heidelberg (2017)
35. Panasonic Corporation: Specifications NCR18650B (2018)
36. Kokam Co., Ltd.: Specification for SLPB8643128H5 (2010)
37. Ladous, R.: Hydrogen for powering aircraft - Roadmap becomes tangible: HEAVEN project. E2Flight conference (2020)
38. Hydrogen-powered Aviation: A Fact-based Study of Hydrogen Technology, Economics, and Climate Impact by 2050, First edition edn. Publications Office of the European Union, Luxembourg (2020). https://doi.org/10.2843/471510